

Supplemental Materials

Isolated Whole Heart Preparation

All procedures were approved by the Office of Research and Integrity Assurance at Georgia Institute of Technology in accordance with the provisions of the USDA Animal Welfare Act Regulations and Standards, PHS policy, conforming to the current Guide for Care and Use of Laboratory Animals. Before deep anesthesia, (Charles River) Hartley Guinea Pigs (female 20 - 22 months) were lightly anesthetized with ketamine/xylazine/acepromazine (17/9/0.9 mg/kg), deeply anesthetized with 3-5% isoflurane mixed with oxygen for induction, and approximately 1-3% for maintenance of deep anesthesia. Five minutes before euthanasia, an intravenous injection of heparin was given (300 U/Kg). Hearts were excised via left thoracotomy, under deep anesthesia. Following excision, hearts were perfused retrogradely via the aorta with warm Tyrode's solution (37 ± 0.5 °C) for 3 minutes and gassed with a mixture of 95% O₂ and 5% CO₂ to expel all the blood and prepare the hearts for perfusion with cold cardioplegic solution, also gassed with a mixture of 95% O₂ / 5% CO₂ to induce cardiac stasis protecting the myocardium, while hearts are transferred to our optical mapping lab (within 15 minutes). The Tyrode's solution contained in mmol/L NaCl 124, KCl 4.0, NaHCO₃ 16, NaH₂PO₄·H₂O 1.2, MgCl₂·6H₂O 1.0, CaCl₂ 1.8, dextrose 5.6. For the optical mapping setup, the hearts were immersed in a heated oval chamber kept at (37 ± 0.5 °C) and Langendorff-perfused with Tyrode's solution gassed with a mixture of 95% O₂ and 5% CO₂. The pressure was maintained at 65 - 70 mmHg. The pH was adjusted to 7.4. Contraction motion was suppressed by (\pm) - Blebbistatin (Cayman Chemicals) at Tyrode's concentration of 1.8 μ M, previously prepared as a stock solution dissolved with DMSO at the ratio of 5 mg/ml.

For optical mapping, we used V_m sensitive dye JPW-6003 (Potentiometric Probes), 0.25 mg of the dye per whole GP heart, previously prepared as a stock solution dissolved with ethanol at the ratio of 20 mg/ml. The dye was injected as a bolus in the cannulated aorta over the course of 3 minutes in small injection intervals, not interfering with the flow rate. The total accommodation time for the heart, including dye staining before taking initial measurements, was at least 30 minutes. Drugs were added at around one hour mark after heart cannulation to the heated Tyrode's solution. HCQ was added to the Tyrode in the concentration of 1000 ng/mL (upper therapeutic dose), previously dissolved in small Tyrode volume free of organic solvents, and steered on a hot plate kept at 35 °C for 15 minutes. AZM was added to the Tyrode

30 in a concentration of 500 ng/ml (upper therapeutic dose), previously dissolved with DMSO at a ratio of 5
31 mg/ml, and steered on a hot plate kept at 35 °C for 15 minutes in small Tyrode volume free of organic
32 solvents.

33 **Optical Mapping Setup**

34 Two red LEDs with the center wavelength at 660 nm were used as light sources for the V_m dye excitation,
35 driven from a stabilized current source (Plumbus donated from Aleksa Tech). The LED light was
36 collimated with a plano-convex lens (ThorLabs) and band-pass filtered with a 660/10 nm filter (Edmund
37 Optics). Emitted fluorescence was filtered through a 700 nm long-pass filter (Chroma Technology) used on
38 the camera side. Fluorescence signals were acquired with an EMCCD camera (Evolve 128, Photometrics)
39 at 128 x 128 pixels, digitized at 16-bits, acquired at 500 FPS, and transferred to a PC via real-time
40 uninterrupted data transfer. A custom acquisition program was used for camera control.

41 **Experimental Protocol**

42 We performed experiments in 12 arterially perfused *ex-vivo* GP hearts: control with no drugs (N = 2),
43 HCQ alone (N = 2), AZM alone (N = 2), and combination of HCQ and AZM (N = 6). For each experiment,
44 optical mapping recordings were made under a steady-state restitution protocol.⁵⁶ The hearts were burst
45 paced from the apex, starting at a cycle length (CL) of 350 ms, decreasing in 5 - 20 ms steps down to the
46 appearance of conduction block or ventricular arrhythmia. The number of burst pacing stimuli at each
47 CL was 40 - 50 beats, allowing sufficient time to reach the steady-state. Each experiment lasted 5 - 6
48 h, and the time it took for drug effects to reach the plateau in the APD prolongation was around 2 - 3 h
49 after administration of the drugs or 3 - 4 h from the beginning of the experiment. Restitution protocols
50 were repeated every 30 min. For the control group of two GP hearts with no drugs, restitution protocols
51 were validated, showing no significant variation in APD values across different CLs throughout the entire
52 duration of the experiments exceeding 6 hours (Figure 2 and Table 1). Also, for each experiment with the
53 added drug(s), two restitution recordings were made before HCQ and/or AZM were infused, at around
54 1 h experiment mark, and compared with the control experiments to ensure no physiological difference
55 among hearts (Table 1 and 2).

56 External bipolar stimuli (World Precision Instruments) of 3 – 5 ms in duration and with the stimulating
57 current at twice the pacing threshold of 3 - 5 mA were applied from the apex. A down-sweep pacing

58 protocol with the pacing cycle length (CL) starting from 350 ms was applied, with the CL gradually
59 shortened in decreasing steps ranging from 5 to 25 ms. For each CL, under the steady-state conditions, 40
60 - 50 beats were recorded. The programming sequence was coordinated with the internal camera trigger
61 clock to control and sync each pacing stimulus's onset. This method allowed us to perform ensemble
62 averaging (image stacking)⁵⁷ to increase the signal-to-noise ratio, avoiding using stronger Spatio-temporal
63 filtering, which may leave undetected small beat to beat APD differences, by over smoothing AP signal in
64 time and space. For each pixel, a signal consisting of 40 - 50 recorded beats was split into even and odd
65 beat sequences, followed by individual stacking of signal sequences.

66 **Experimental Data Processing**

67 All experimental data processing was performed in MATLAB (Mathworks, version 2020) and Julia
68 programming language. The workflow for optical mapping data processing consists of a baseline removal
69 for each pixel signal⁵⁸, up-sampling to 2000 Hz, uniform Gaussian filtering with 3 x 3 spatial and 1 x 5
70 temporal kernel sizes, and the stacking procedure.⁵⁷ APD maps were obtained by calculating each pixel
71 signal as the time duration between action potential (AP) rise to 50% in amplitude until it reaches 75%
72 re-polarization level, APD75%, for both even and odd beat individually. From even and odd APDs values
73 across every pixel of the image sequence, APD spatial dispersion maps were obtained as the difference
74 between even and odd APD map.

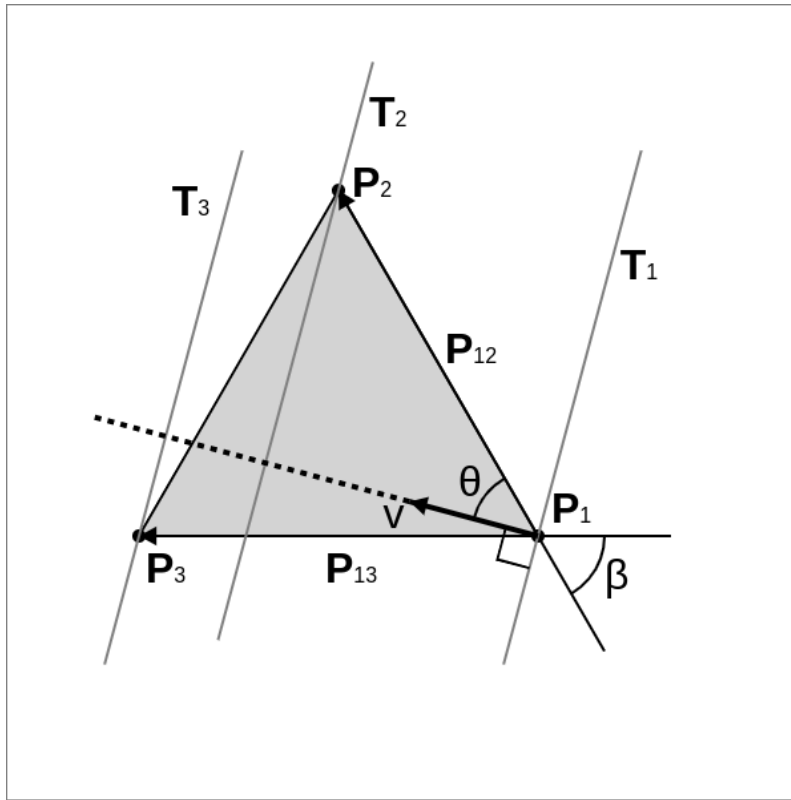
75 The range for color-coding of APD values in APD maps was performed in a standard statistical
76 approach. For APD values of even and odd beats maps, the colormap range corresponds to 3rd to 97th
77 percentile of APD values, obtained for each CL. For the APD spatial dispersion maps (Δ APD), a different
78 colormap was used with emphasis to represent zero values with a white color, representing a nodal line
79 separating regions alternating out of phase.

80 **Three-Point Conduction Velocity Measurement**

81 Our goal is to measure the velocity of an activation wavefront, which, in case of two-dimensional excitable
82 tissues, is equal to the conduction velocity (CV). In general, CV is inversely proportional to the spatial
83 gradient of the activation time (∇t), where $t(x, y)$ is the activation time for the current wavefront at pixel
84 (x, y) . One technique to calculate CV is to choose a rectangular region Ω , use the least square method
85 to fit a plane to t over Ω , and finally calculate ∇t based on the slope of the plane. This technique is very
86 sensitive to noisy and bad pixels, which are not uncommon in optical mapping recordings.

87 In this paper, we use a three-point CV measurement method, where the activation time at only three
 88 non-colinear points are used to measure CV. The main benefits are the ease of use (there is a closed
 89 formula, see below) and the fact that it is less difficult to find three good points than a uniformly acceptable
 90 rectangular region. It should be noted that the final result is mathematically equivalent to finding the
 91 gradient (as above), but we opted to use a trigonometric argument for clarity.

92 Let's the three points be \mathbf{P}_1 , \mathbf{P}_2 , and \mathbf{P}_3 (Figure 1). We assume the activation wavefront is straight and
 93 uniform (the best we can do with three points) and hits \mathbf{P}_1 at $t = t_1$ (line \mathbf{T}_1 in the figure), \mathbf{P}_2 at $t = t_2$, and
 94 \mathbf{P}_3 at $t = t_3$.



Supplemental Figure 1

We define $\mathbf{P}_{12} = \mathbf{P}_2 - \mathbf{P}_1$ and $\mathbf{P}_{13} = \mathbf{P}_3 - \mathbf{P}_1$. Let β be the angle between \mathbf{P}_{12} and \mathbf{P}_{13} ,

$$\beta = \cos^{-1} \left(\frac{\mathbf{P}_{12} \cdot \mathbf{P}_{13}}{|\mathbf{P}_{12}| |\mathbf{P}_{13}|} \right)$$

95 and \mathbf{v} the velocity vector. We want to find \mathbf{v} given the three points \mathbf{P}_1 , \mathbf{P}_2 , \mathbf{P}_3 , and the corresponding
 96 activation times, t_1 , t_2 , and t_3 . Let $v = |\mathbf{v}|$ be the velocity magnitude and θ the angle between \mathbf{v} and \mathbf{P}_{12} .
 97 Then, our goal is to find v and θ .

Let's define

$$\mu_{12} = \frac{t_2 - t_1}{|\mathbf{P}_{12}|},$$

and

$$\mu_{13} = \frac{t_3 - t_1}{|\mathbf{P}_{13}|}.$$

We have,

$$(t_2 - t_1)v = \mathbf{P}_{12} \cdot \frac{\mathbf{v}}{v},$$

noting that \mathbf{v}/v is the unit vector in the direction of \mathbf{v} . Expanding the inner product,

$$(t_2 - t_1)v = |\mathbf{P}_{12}| \cos(\theta).$$

Therefore,

$$\mu_{12}v = \cos(\theta).$$

Similarly,

$$\mu_{13}v = \cos(\beta - \theta).$$

Substituting the formula for the cosine of the difference of two angles,

$$\mu_{13}v = \cos(\beta) \cos(\theta) + \sin(\beta) \sin(\theta).$$

Therefore,

$$\frac{\mu_{13}}{\mu_{12}} = \cos(\beta) + \sin(\beta) \tan(\theta).$$

Rearranging, we obtain the formula for calculating θ ,

$$\tan(\theta) = \frac{\mu_{13}/\mu_{12} - \cos(\beta)}{\sin(\beta)}.$$

Using $\cos(\theta) = 1/\sqrt{1 + \tan^2(\theta)}$ and $v = \cos(\theta)/\mu_{12}$, we have the formula for v ,

$$v = \frac{\sin(\beta)}{\sqrt{\mu_{12}^2 + \mu_{13}^2 - 2\cos(\beta)\mu_{12}\mu_{13}}}.$$

⁹⁸ Substituting β , μ_{12} and μ_{13} , we can express v in terms of \mathbf{P} s and ts ,

$$v = \frac{\sqrt{|\mathbf{P}_{12}|^2 |\mathbf{P}_{13}|^2 - (\mathbf{P}_{12} \cdot \mathbf{P}_{13})^2}}{|(t_3 - t_1)\mathbf{P}_{12} - (t_2 - t_1)\mathbf{P}_{13}|}$$

99 Intuitively, this equation should be symmetrical on the three points. In fact, it is symmetrical! Let x_i and y_i
 100 be the coordinates of \mathbf{P}_i . We can calculate v^2 as

$$v^2 = \frac{\det \begin{pmatrix} x_1 & x_2 & x_3 \\ y_1 & y_2 & y_3 \\ 1 & 1 & 1 \end{pmatrix}^2}{\det \begin{pmatrix} x_1 & x_2 & x_3 \\ t_1 & t_2 & t_3 \\ 1 & 1 & 1 \end{pmatrix}^2 + \det \begin{pmatrix} y_1 & y_2 & y_3 \\ t_1 & t_2 & t_3 \\ 1 & 1 & 1 \end{pmatrix}^2}$$

101 The proof that the different formulas for calculating v are equal is based on a straightforward, but rather
 102 cumbersome, expansion and comparison of the formulas.

103 Simulation and Numerical Methods and Results

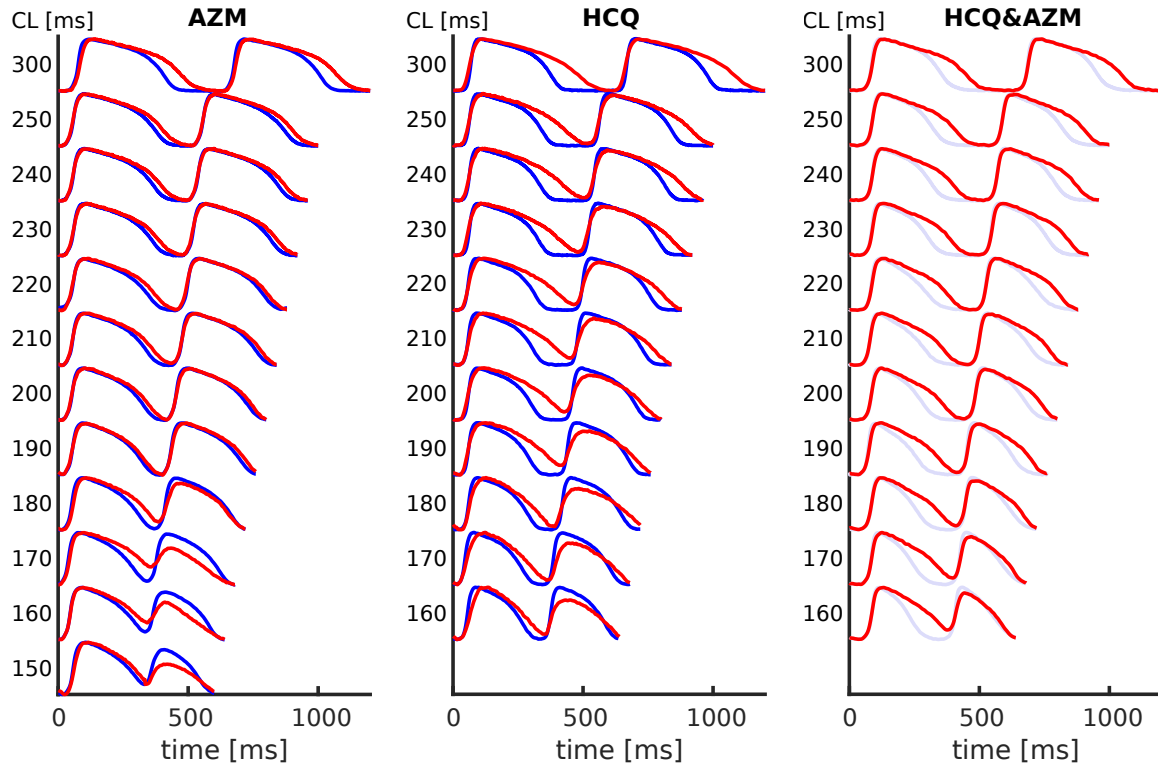
104 Simulations using mathematical models were performed in WebGL. For the numerical studies, we first
 105 used a mathematical cardiac cell model for GP ionic currents⁵⁹ to compare with our experimental results
 106 (Supplemental Figure 3). To simulate the drug effects, the conductance of ion channels affected was
 107 reduced as previously reported in patch-clamp experiments^{60,61}. The effects of HCQ alone were simulated
 108 by reducing the sodium current (I_{Na}) by $25 \pm 4\%$, the rapid delayed rectifier potassium current (I_{Kr}) by
 109 $65 \pm 7\%$, the slowly activating potassium currents (I_{Ks}) by $7 \pm 6\%$, inwardly rectifying potassium current
 110 (I_{K1}) by $86 \pm 7\%$, and lastly, the L-type channel was blocked by $9 \pm 3\%$ which affects the L-type calcium
 111 current (I_{CaL}), and sodium and potassium currents I_{CaNaL} and I_{CaKL} as well. Similarly, the AZM drug
 112 effects were simulated reducing I_{Na} by $15 \pm 3\%$, I_{Kr} by $20 \pm 3\%$, I_{Ks} by $6 \pm 3\%$, I_{K1} by $4 \pm 2\%$ and the
 113 L-type channel by $7 \pm 5\%$. The effects of combined HCQ and AZM were simulated reducing the I_{Na} by
 114 $23 \pm 2\%$, I_{Kr} by $65 \pm 7\%$, I_{Ks} by $9 \pm 2\%$, I_{K1} by $84 \pm 7\%$, and the L-type channel by $5 \pm 3\%$.

115 Statistical Analysis

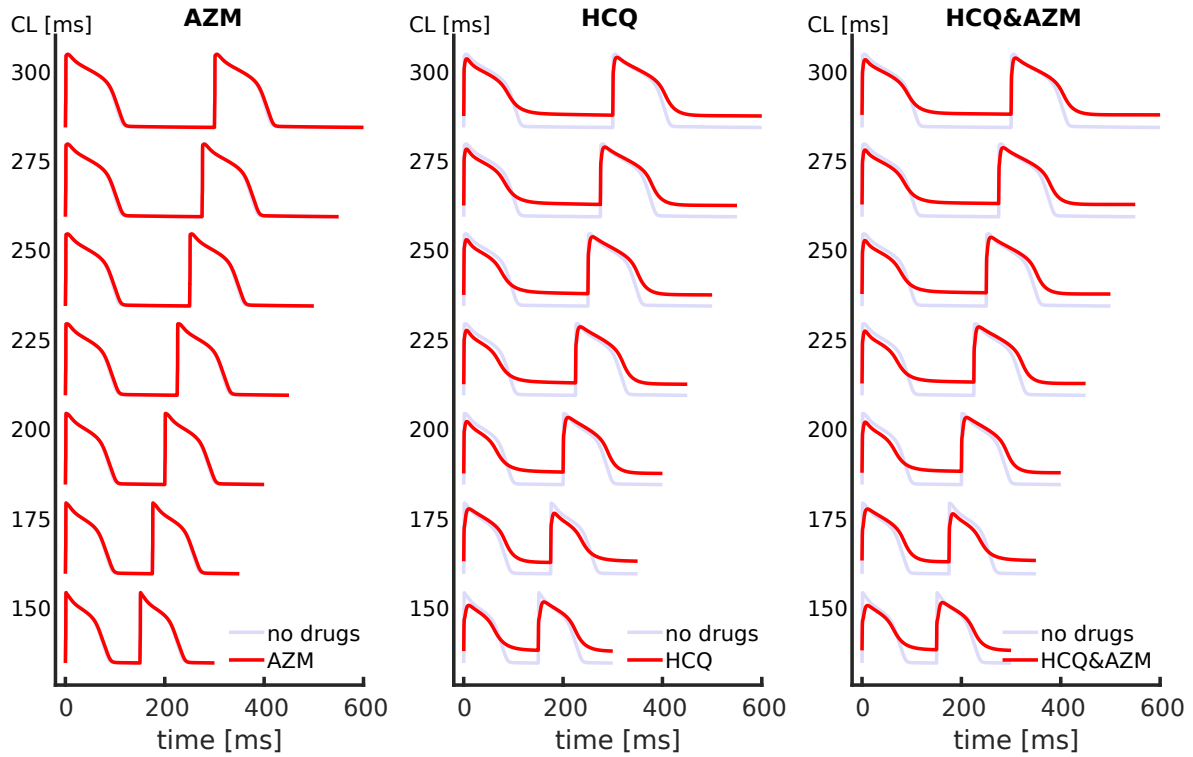
116 Descriptive data are presented as absolute numbers and percentages or means and SDs. Significance of
 117 differences between treatment groups and the control groups was assessed using Student's t test. Paired t
 118 test was used to determine significance between the control group and the hearts treated with the drugs. P
 119 values less than 0.05 were considered significant. Analyses were conducted using MATLAB software
 120 (version 2020, Mathworks)

121 **Data Availability**

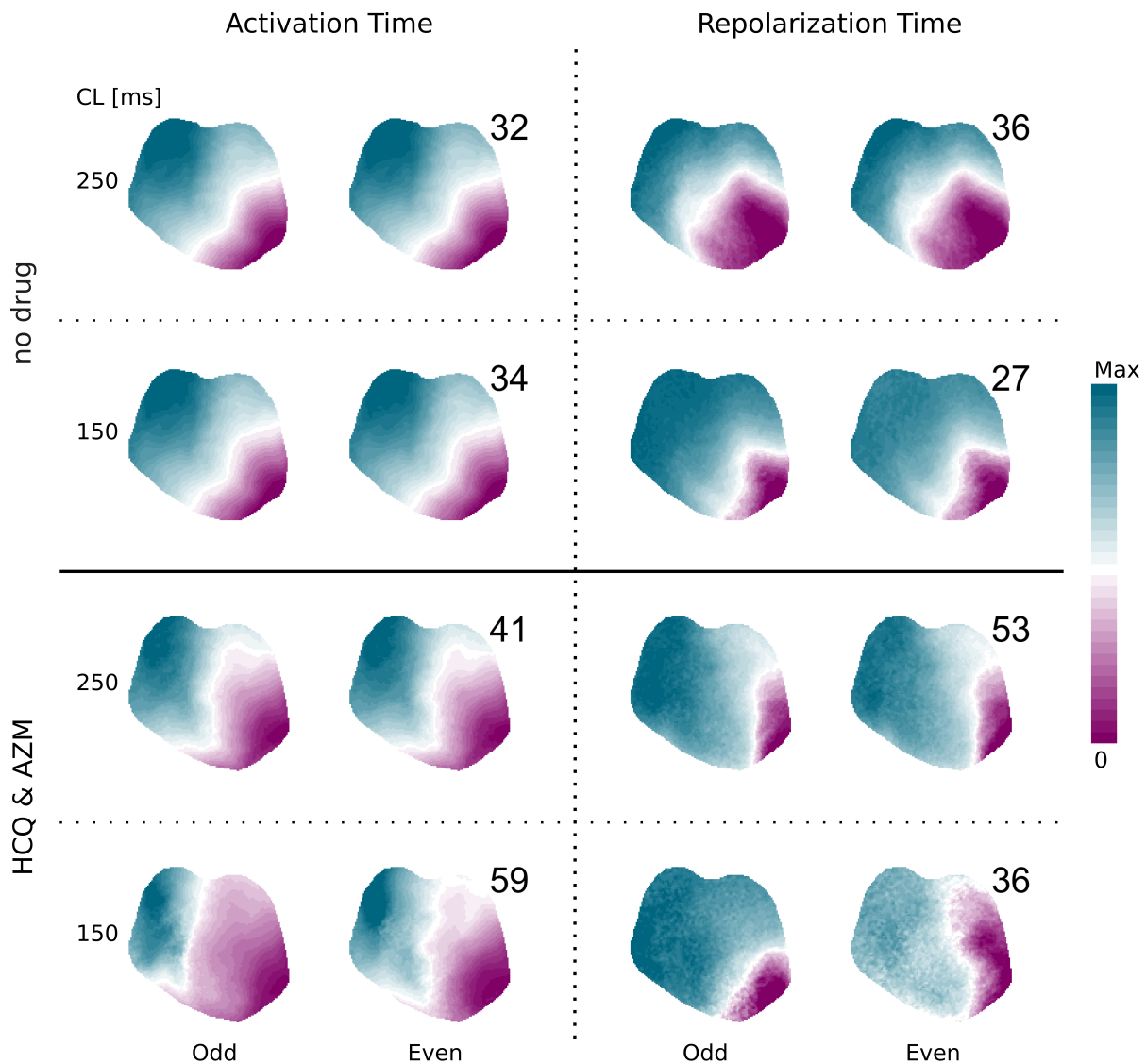
122 The data that support the findings of this study are available from the corresponding author upon reasonable
123 request.



Supplemental Figure 2. | Comparison of optical APs of HCQ and AZM and combination of HCQ and AZM. The APs are from a single pixel in the left ventricle obtained from raw data upsampled from 500 to 2000 samples per second, filtered with a Gaussian filter of 3 x 3 spatial and 1 x 7 temporal kernel sizes, and ensemble averaged in time for each CL. Blue color show optical APs before the drugs and red after the drugs were added.



Supplemental Figure 3. | Comparison of APs of HCQ and AZM and combination of HCQ and AZM in GP model. The resting membrane potential is elevated with HCQ and combination of HCQ and AZM across all CLs. The model replicates AP alternans and APD prolongation. Light blue color shows the AP before the drugs were added.



Supplemental Figure 4. | Comparison of activation wavefront maps and repolarization waveback maps for no drug vs HCQ&AZM in GP experiments at two different periods of stimulation 250 and 150 ms, for even and odd beats. The repolarization follows the activation pattern for no drug, with no alternans present as the period of stimulation decreases. With the drugs, activation and repolarization (inactivation) patterns are very different, showing an enhanced irregular dispersion of repolarization. There is a noticeable prolongation in activation and deactivation times and differences between even and odd beat produce complex dispersion of repolarization shown by the discordant alternans in Figure 1 of the manuscript. The numbers indicate the time in ms until 97% of the tissue is activated, and time until 97% is deactivated, measured at 75% of repolarization level. Time is indicated in color from magenta to turquoise, with a white color corresponding to average activation and average deactivation time.

The restitution curve fit to $A + Be^{-DI/\tau}$

#	Group	A_b	A_a	B_b	B_a	τ_b	τ_a
1	CONTROL	26.7 ± 9.8	30.0 ± 13.0	171.1 ± 6.4	149.0 ± 11.0	101.0 ± 14.0	55.3 ± 5.5
2	CONTROL	13.0 ± 12.0	1.0 ± 25.0	161.0 ± 16.0	171.0 ± 20.0	98.0 ± 10.0	64.0 ± 13.0
3	HCQ	37.8 ± 2.7	5.0 ± 41.0	128.5 ± 3.4	309.0 ± 28.0	86.4 ± 5.6	81.0 ± 17.0
4	HCQ	17.0 ± 12.0	4.0 ± 27.0	168.3 ± 7.4	258.0 ± 21.0	95.3 ± 9.3	70.0 ± 15.0
5	AZM	60.3 ± 7.5	-1.0 ± 29.0	123.9 ± 4.1	228.0 ± 25.0	86.0 ± 11.0	64.0 ± 14.0
6	AZM	23.0 ± 10.0	-45.0 ± 42.0	107.5 ± 6.2	219.0 ± 31.0	85.0 ± 13.0	57.0 ± 17.0
7	HCQ/AZM	16.0 ± 19.0	10.0 ± 23.0	142.0 ± 20.0	295.0 ± 29.0	53.4 ± 8.4	83.0 ± 12.0
8	HCQ/AZM	27.0 ± 10.0	-77.0 ± 40.0	136.4 ± 7.3	315.0 ± 25.0	73.7 ± 8.0	55.8 ± 6.3
9	HCQ/AZM	9.2 ± 8.6	-4.0 ± 28.0	192.4 ± 5.4	277.0 ± 13.0	83.6 ± 8.4	102.0 ± 33.0
10	HCQ/AZM	-7.0 ± 16.0	-81.0 ± 49.0	208.0 ± 12.0	271.0 ± 37.0	102.4 ± 8.8	56.1 ± 9.0
11	HCQ/AZM	35.0 ± 11.0	23.0 ± 18.0	206.0 ± 12.0	288.0 ± 16.0	154.0 ± 42.0	137.0 ± 25.0
12	HCQ/AZM	16.0 ± 12.0	-3.0 ± 40.0	190.0 ± 15.0	219.0 ± 34.0	136.0 ± 15.0	64.0 ± 11.0

Supplemental Table 1. Restitution curve fit parameters. Fit parameters for the APD steady state vs. diastolic interval (DI), before (*b*) and after (*a*) the treatment with drugs. For the control experiments, the fit curves are at the beginning (between 30 and 60 minutes from heart cannulation) and six hours later from the time when heart was perfused with warm Tyrode solution.

124 **References**

- 125 **56.** Uzelac I, Ji YC, Hornung D, et al. Simultaneous quantification of spatially discordant alternans in
126 voltage and intracellular calcium in langendorff-perfused rabbit hearts and inconsistencies with models
127 of cardiac action potentials and ca transients. *Front Physiol* 2017;8:819.
- 128 **57.** Uzelac I, Fenton FH. Robust framework for quantitative analysis of optical mapping signals without
129 filtering. In *2015 Computing in Cardiology Conference (CinC)*. IEEE, 461–464.
- 130 **58.** Uzelac I, Iravanian S, Fenton FH. Parallel acceleration on removal of optical mapping baseline
131 wandering. In *2019 Computing in Cardiology (CinC)*. IEEE, Page–1.
- 132 **59.** Livshitz LM, Rudy Y. Regulation of ca²⁺ and electrical alternans in cardiac myocytes: role of camkii
133 and repolarizing currents. *Am J Physiol-Heart C* 2007;292:H2854–H2866.
- 134 **60.** Sánchez-Chapula JA, Salinas-Stefanon E, Torres-Jácome J, Benavides-Haro DE, Navarro-Polanco RA.
135 Blockade of currents by the antimalarial drug chloroquine in feline ventricular myocytes. *J Pharmacol*
136 *Exp Ther* 2001;297:437–445.
- 137 **61.** Wang G, Tian X, Lu CJ, et al. Mechanistic insights into ventricular arrhythmogenesis of hydroxy-
138 chloroquine and azithromycin for the treatment of covid-19. *bioRxiv* 2020;.